RESEARCH ARTICLE
doi: 10.2306/scienceasia1513-1874.2024.030

ScienceAsia 50 (1): 2024: ID 2024030: **1–9**

Cotton tree (*Bombax ceiba* L.) flower stamen extract: Turning a food ingredient into a reducing agent for the green synthesis of silver nanoparticles

Sakoolrud Raunmoon[a], Supakid Sachak[a], Waranya Thong-in[a], Boonyakorn Sonkhayan[a], Pitak Nasomjai[a], Phichaya Khamai[b], Arthid Thim-uam[b], Paideang Khwanchai[c], Chee O. Too[a], Widsanusan Chartarrayawadee[a,*]

[a] Division of Chemistry, School of Science, University of Phayao, Phayao 56000 Thailand
[b] Division of Biochemistry, School of Medical Sciences, University of Phayao, Phayao 56000 Thailand
[c] Division of Food Science and Technology, School of Agriculture and Natural Resources, University of Phayao, Phayao 56000 Thailand

[*]Corresponding author, e-mail: widsanusan.ch@up.ac.th

Received 7 Dec 2022, Accepted 28 Nov 2023
Available online 10 Mar 2024

ABSTRACT: Cotton tree (*Bombax ceiba* L.) flower stamen has been used widely as a northern Thai food ingredient. In this work, microwave extraction was applied to obtain the *Bombax ceiba* L. (BOMBAX) flower stamen extract for use as a reducing agent in the green synthesis of silver nanoparticles (AgNPs). The concentration of BOMBAX used was in the range of 0.05 to 0.25 wt%. Quasi-spherical and semi-rectangular shapes of AgNPs were obtained. The synthesized AgNPs showed a high mean zeta potential value of more than −30 mV, indicating the long-term stability and superior dispersity of AgNPs due to the repulsion of negative charges. Furthermore, the antibacterial potency of the synthesized AgNPs affords a good inhibition zone for both gram-negative and gram-positive bacteria, especially the gram-negative and antibiotic-resistant bacteria *Pseudomonas aeruginosa*, showing an inhibition zone diameter of 19.4 ± 0.4 mm compared with that of chlophenicol (13.0 ± 0.0 mm). This result suggests that the synthesized AgNPs present good colloidal stability and show good potential as an antibacterial agent for antibiotic-resistant bacteria, especially *P. aeruginosa*.

KEYWORDS: green synthesis, silver nanoparticles, cotton tree, *Bombax ceiba* L., antibacterial

INTRODUCTION

Bombax ceiba L. (BOMBAX) recognized as the "sumbal tree" or "silk cotton tree" is an Asian tropical plant, also known as the cotton tree or red cotton tree, due to the physical characteristics of red flowers and white, cotton like fibers. This plant has been used in the wooden furniture manufacturing industry and as a spice ingredient in cooking such as the main ingredient in "nam ngiao" spicy noodle soup in the northern part of Thailand. In ancient times, *B. ceiba* L. was called the "silent doctor" because every part of it, including the flowers, stem, bark, and leaves, exhibits numerous pharmacological properties that can be used in many medicinal applications [1]. Phytochemical screening has indicated that there are a variety of useful phytochemicals present in the flowers such as polyphenols, alkaloids, flavonoids, coumarins, glycosaponins, tannins, terpenoids, and cardiac glycosides [2].

Green synthesis of metal nanoparticles is popularly used in many scientific fields, including pure sciences and applied sciences involving nanoscale synthesis of metals. Green synthesis is a process that involves the reduction of metal nanoparticles using plant extracts instead of chemical-reducing agents. Nowadays, green synthesis has become more popular in an increasing number of research areas [3]. The replacement of physical and chemical synthesis by green synthesis has become more attractive due to environmental concerns such as the use of toxic and harmful chemicals, high energy consumption, and sustainability. Most of the metal nanoparticles developed through green synthesis are silver (AgNPs) [4, 5], gold (AuNPs) [6, 7], copper (CuNPs) [8, 9], copper oxide (CuONPs) [10, 11], iron (FeNPs) [12, 13], iron oxide (IONPs) [14, 15], and palladium (PdNPs) [16, 17]. There have been several studies on the use of green synthesis of AgNPs employing many kinds of plant extracts as reducing and stabilizing agents; these studies have shown antibacterial activity effecting both gram-positive and gram-negative bacteria [18, 19]. For example, Ajitha et al [18] used the *Tephrosia purpurea* leaf extract to synthesize nano-scale AgNPs for antimicrobial activity. The *Hagenia abyssinica* (Bruce) J.F. Gmel plant leaf extract has been utilized for green synthesis of AgNPs; antibacterial and antioxidant activities were investigated [20]. Extract of *Eugenia roxburghii* DC. was used for the synthesis and characterization of AgNPs, and the activity against biofilm-producing bacteria was also studied [21]. In another study, Taghavizadeh et al [22] utilized *Helichrysum graveolens* extract for green synthesis of AgNPs, which showed anticancer activity against the colon cancer cell line (C26) and also acted as a green catalyst for the acceleration of methylene orange degradation. Ranjan et al [23] reported synthesis of AgNPs using the extract of *Nigella*

sativa. The results showed an antibacterial reaction of AgNPs against urinary tract infection causing bacteria. The synthesized AgNPs using neem leaf extract demonstrated an optimum surface plasmon resonance (SPR) behavior due to the presence of a high concentration of diterpenoids in the extract. Potential biosensing and photocatalytic applications were also reported in this work [24]. Microwave synthesis has been employed in the formation of spherical-like AgNPs using curcumin biomaterial as a reductant and stabilizer for improving antibacterial properties against *Staphylococcus aureus* and *Escherichia coli* natural rubber/Ag composite materials [25].

The aim of the current work was to perform the green synthesis of AgNPs by using *B. ceiba* L. flower stamen extract (BOMBAX) as a reducing and stabilizing agent for the first time. The resultant AgNPs were characterized, and their formation, stability, size, shape, and antibacterial activity were observed.

MATERIALS AND METHODS

Chemicals and materials

AR-grade silver nitrate ($AgNO_3$) was purchased from Labscan (RCL Labscan Limited, Bangkok, Thailand). The dried flower stamen of the cotton tree (*B. ceiba* L.) was purchased from a local market in Phayao province, Thailand. The nutrient agar (Muller Hinton agar (MHA) and Muller Hinton broth (MHB) were purchased from HiMedia Laboratories (HiMedia Laboratories Pvt. Ltd., Mumbai, India). Deionized water (RCL Labscan Limited, Bangkok, Thailand) was used in all the experiments.

Preparation of flower stamen extract of *B. ceiba* L.

The 100 g of dried flower stamen of *B. ceiba* L. were cut into small pieces in a Moulinex blender and were heated in the microwave for 15 min at 130 W with deionized water. The ratio of dried flower stamen to deionized water was 1 g:10 ml. The obtained solution was filtered until it became clear and then lyophilized to obtain the extracted powder of *B. ceiba* L. (BOMBAX) that was brown in color.

Synthesis of silver nanoparticles

The green synthesis of AgNPs using BOMBAX as a reducing and stabilizing agent was performed as follows: Solution of silver nitrate 10 ml, 0.025 wt% of $AgNO_3$ was added to 10 ml of BOMBAX solution. The concentration of BOMBAX in the mixture was prepared as follows: 0.05, 0.10, 0.15, and 0.25 wt%. The solution mixture was then stirred until it became homogeneous. The reaction mixture was stirred overnight for 12 h at an ambient temperature, and then the temperature was increased to 80 °C for 1 h in the final step. The AgNP formation was observed by the appropriate color change from light brown to dark brown depending on the BOMBAX concentration used as a reducing agent. AgNP colloidal solution was kept away from light at ambient temperature prior to use.

Antimicrobial activity

The antibacterial activity of the obtained AgNPs was assessed using the disc diffusion method following standards and guidelines from the Clinical Laboratory Standards Institute (CLSI). The overnight-grown bacteria used in this study were gram-negative bacteria (*P. aeruginosa*, *Shigella* sp., *S. enteritidis*, *E. coli*, and *K. pneumoniae*) and gram-positive bacteria (*S. aureus* and *E. faecalis*), which were standardized using the McFarland standard (McFarland standard No. 0.5). These microorganisms were collected, cultured, and maintained at the Department of medical microbiology and parasitology, School of Science, University of Phayao, Phayao, Thailand. The bacteria suspensions were diluted 1:10 to obtain 1.5×10^7 colony forming units per milliliter (CFU/ml) and plated on the nutrient agar using sterile cotton buds. Antibacterial testing samples were prepared by adding a small volume (50 µl) of chloramphenicol, NaCl, $AgNO_3$ (0.025 wt%), BOMBAX solution (0.25 wt%), and the different dilutions of obtained biosynthesized AgNPs varied from 0.05, 0.10, 0.15 and 0.25 wt%; these were then dropped onto the antibiotic test plate, sheet, grade MN 827 ATD, 6 mm. Each Petri plate containing nutrient agar was loaded with 4 antibacterial testing samples. The Petri plates were incubated at 37 °C for 18 h and then examined for the appearance of a clear area around the disc by measuring the diameter of inhibition zones using a ruler, which was recorded and expressed in millimeters. The antibacterial activity of AgNPs was compared to the size and diameter of inhibition zones.

Sample characterization

The formation of Ag nanoparticles was observed using a UV-Vis spectrometer (Jusco, V530, Jasco International Co., Ltd., Tokyo, Japan) in dual beam mode. The functional groups on AgNPs were validated using a Fourier-transform infrared (FTIR) spectrometer (Nicolet 6700, Thermo Fisher Scientific, Massachusetts, US). A laser particle sizer (Malvern Zetasizer Nano ZS, Malvern Instruments Limited, Worcestershire, UK) equipped with a He-Ne laser at 633 nm, 4 mW was used to determine particle size and zeta potential at 25 °C through dynamic light scattering (DLS) in backscattering mode. An X-ray diffractometer (Rigaku Miniflex 600 X-ray diffractometer using Cu Kα x-ray radiation, Rigaku Corporation, Tokyo, Japan) was used to obtain the diffraction patterns of the AgNPs on a glass slide. The surface morphology, size, and structural properties of AgNPs were characterized by SEM (SEM, Philips Tecnai 12, FEI Company, Oregon, US).

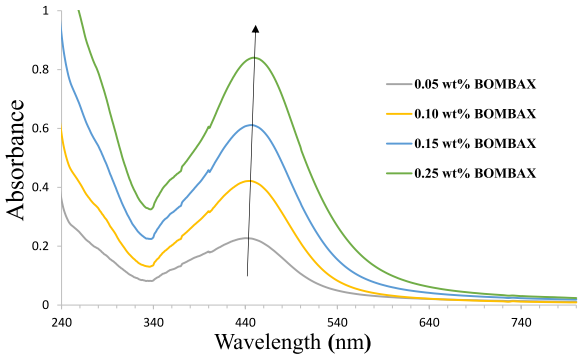

Fig. 1 UV-Vis spectra of AgNPs reduced by BOMBAX with concentration range from 0.05 wt% to 0.25 wt%.

RESULTS AND DISCUSSION

Spectroscopic measurements

The formation of green synthesized AgNPs using *B. ceiba* L. (BOMBAX) extract was investigated using UV-Vis spectroscopy. The synthesis of AgNPs was carried out in a dark room, and the obtained AgNP colloidal solution was kept under dark conditions at ambient temperature to protect the photosensitive nature of the silver until use. AgNP colloidal solutions with different BOMBAX concentrations were characterized with UV-Vis spectroscopy on the first day after heat treatment. The effect of BOMBAX concentration on the formation of AgNPs is shown in the UV-Vis spectra (Fig. 1). The absorbance intensity of the AgNP colloidal solution increases with respect to BOMBAX concentration, which can be interpreted that the formation rate of AgNPs is slower at the lowest concentration of BOMBAX and gradually increases when BOMBAX concentrations are increased. The SPR peaks at a wavelength of around 450 nm for the whole concentration range of BOMBAX indicated the maximum formation of AgNPs and the color became brown. In terms of AgNP shape and the number of SPR bands, the more dimensions that exist for the AgNP shape, the more SPR bands appear [26]. Spherical, rod, and triangular shapes can produce one, two and three SPR bands, respectively. A single SPR band was observed in each concentration of BOMBAX, indicating the spherical shape or quasi-spherical shape of AgNPs [27, 28]. Furthermore, red shifting in the SPR band indicated that a larger particle size was observed with respect to the concentrations of BOMBAX. The peak position between 450–460 nm can also be used to predict AgNP size, which should be approximately 70 nm [29]. The UV-Vis spectroscopy result can be used as evidence of the reduction of silver ions (Ag^+) to AgNPs, which is promoted by the functional groups of phytonutrients in BOMBAX. The phytochemical compounds found in BOMBAX such as flavonoids and phenolic acids are rich in hydroxyl groups (—OH group), which can be associated with electron transfer in the reduction of Ag^+ to silver (Ag^0), leading to the formation of silver nuclei and production of silver nanoparticles (AgNPs) [30].

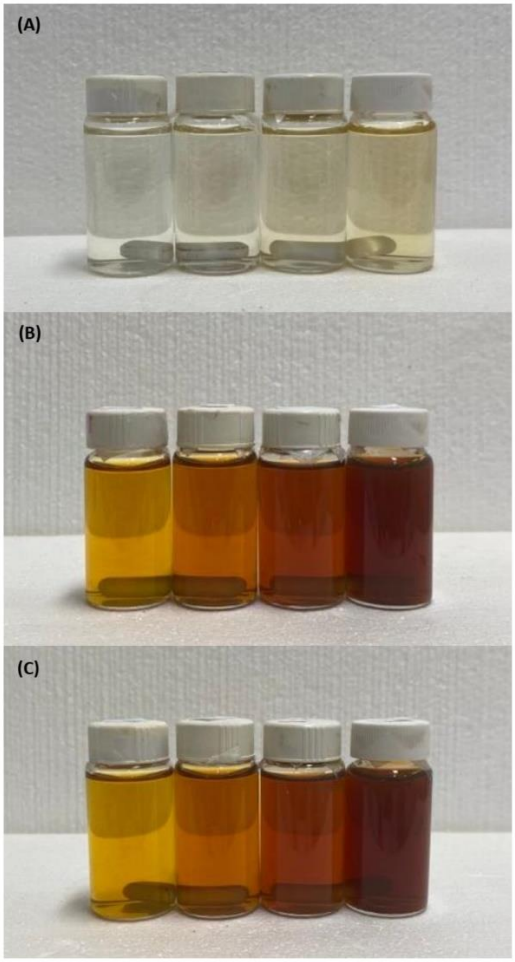

Fig. 2 Changes in color intensity of AgNP aqueous colloidal solution reduced by BOMBAX before reduction (A), after overnight reduction (B), and after overnight reduction followed by heating at 80 °C for 1 h, then left aside for 24 h (C). From left to right, BOMBAX concentration starts from 0.05 to 0.25 wt%.

Fig. 2 shows the series of color intensity increases in the $AgNO_3$ aqueous solutions reduced by BOMBAX extract: before reduction, after overnight reduction, and after overnight reduction followed by heating at 80 °C for 1 h. The samples that were left for over 24 h show more intense changes in colors in all the series from the beginning (left) to the end (right) of the synthesis steps as shown in Fig. 2(A–C). Furthermore, the color intensity of the final products after the reduction shows the most intense color changes from yellow to dark brown (Fig. 2C) when compared with $AgNO_3$ aqueous solution reduced by BOMBAX

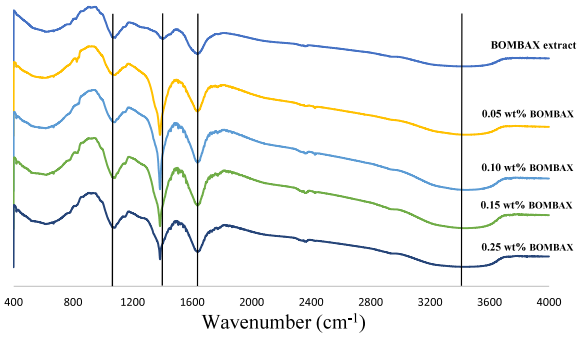

Fig. 3 Changes in color intensity of AgNP aqueous colloidal solution reduced by BOMBAX before reduction (A), after overnight reduction (B), and after overnight reduction followed by heating at 80 °C for 1 h, then left aside for 24 h (C). From left to right, BOMBAX concentration starts from 0.05 to 0.25 wt%.

before reduction (Fig. 2A) and after overnight reduction (Fig. 2B). This result suggests that AgNPs can be successfully synthesized using BOMBAX extract and this can be confirmed based on the surface plasmon resonance absorption.

Fig. 3 shows FTIR spectra of pure BOMBAX and dried powder obtained from AgNP colloidal solutions reduced using BOMBAX at different concentrations. A broad absorption peak is observed at around 3450 cm^{-1}, which is attributed to the OH functional group of alcoholic and phenolic compounds. Frequency of the amide I band is found in the range between 1600 and 1700 cm^{-1}, which is mainly associated with the stretching vibrations of C=O. Peaks at 1639 cm^{-1} represent a C=O stretch of the carboxylic/carbonyl group. Peaks at 1384 cm^{-1} indicate the bending of C–H asymmetric in CH_2 and CH_3 groups. Moreover, the peak at 1070 cm^{-1} represents C–O stretching. FTIR spectra revealed the different types of functional groups (–OH, C–H, C=O, and C–O) on AgNPs that are involved with bio-reduction and stabilization of AgNPs. The similarity of the IR spectra between BOMBAX and AgNPs indicates that the compounds found in BOMBAX existed in all samples. The marked shifts observed from the FTIR results confirm that the AgNPs were biosynthesized and coated with different functional groups of phytochemicals found in Bombax.

X-ray diffraction

X-ray diffraction (XRD) is a characterization technique used in materials science to investigate the primary crystallographic structure of a material. AgNP powder (after heat treatment) reduced by BOMBAX at the different concentrations was subjected to analysis of their crystalline structure; the result in Fig. 4 confirms that all AgNP samples reduced by BOMBAX extract are crystalline in nature. The XRD patterns showed peaks at (2θ) around 38°, 44°, 64°, and 78°, which could be indexed as (111), (200), (220), and (311) Bragg reflections, respectively. The sets of these diffraction peaks agreed with the standard data file (JCPDS No. 04-0783, International Centre for Diffraction Data (ICDD), Newton Square Pennsylvania, USA) of the Joint Committee on Powder Diffraction Standards and were consistent with other literature reports [31]. However, other additional unassigned peaks, especially found in the XRD patterns of AgNPs reduced by BOMBAX at the concentration of 0.25 wt%, are also observed; this may be due to the formation of the crystalline metallo-protein in BOMBAX extract [32] or $AgNO_3$, which had not been reduced and remained in the sample [33].

Table 1 Mean zeta potential values and mean particle sizes (1st peak and 2nd peak in nm) of AgNP colloidal solutions obtained from BOMBAX bio-reduction (after heat treatment) at different concentrations ranging from 0.05 to 0.25 wt%.

Concentration of BOMBAX (wt%)	Mean zeta potential (mV)	Mean particle size (1st peak-nm)	Mean particle size (2nd peak-nm)
0.05 wt% BOMBAX	–34.2 ± 0.4	4.3 ± 0.0	73.2 ± 36.4
0.10 wt% BOMBAX	–30.9 ± 1.6	5.3 ± 0.4	80.6 ± 41.5
0.15 wt% BOMBAX	–32.9 ± 1.8	7.7 ± 1.4	78.7 ± 35.8
0.25 wt% BOMBAX	–30.4 ± 1.6	10.0 ± 1.8	88.3 ± 45.2

Zeta potential and size distribution

Dynamic Light Scattering (DLS) technique was used to determine the zeta potential and size of AgNPs. Particles in a colloidal solution containing a large negative or positive zeta potential value can lead to high stability of the colloidal particles due to their repulsion of each other, resulting in the prevention of coalescence of the colloidal particles. However, at small negative or positive zeta potential values, agglomeration and flocculation can occur due to charge and force minimization allowing particles to come close together [34, 35]. Surprisingly, all synthesized AgNP colloidal solutions show high negative zeta potential values (Table 1), supporting high stability, good colloidal solution, and superior dispersity of AgNPs due to the repulsion of negative charges.

The mean particle sizes of AgNP colloidal solution show polydispersity in nature as shown in Table 1. The mean particle sizes of the 1st and 2nd peaks of AgNPs reduced by BOMBAX at different concentrations are also shown in Table 1. When the concentration of BOMBAX increases, AgNP size also increases. This can be explained by the influence of phytochemicals (triterpenoid saponins, flavonoids, and glycosides) found in BOMBAX in the bio-reduction of AgNPs.

SEM Morphology

An SEM was used to determine the size and morphol-

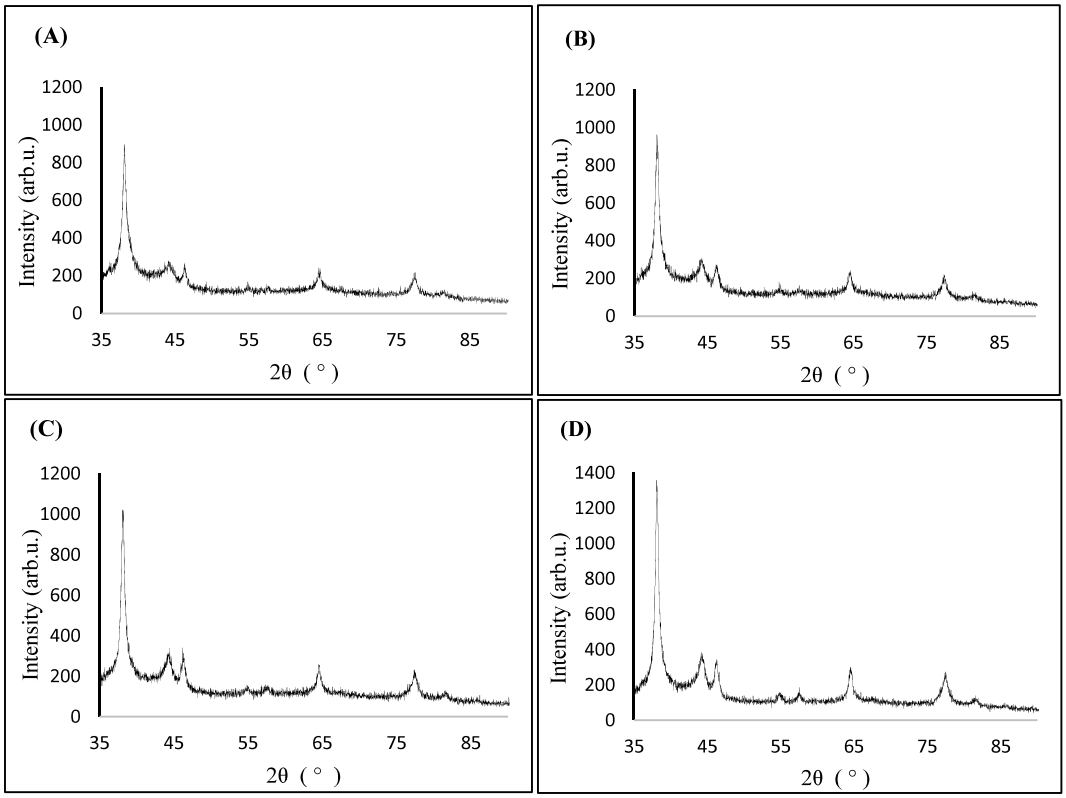

Fig. 4 Powder XRD pattern of AgNPs obtained from AgNP colloidal solution reduced and stabilized by BOMBAX of different concentrations: (A) 0.05 wt%, (B) 0.10 wt%, (C) 0.15 wt%, and (D) 0.25 wt%.

Table 2 Inhibition zone diameters (mm, average value ± standard deviation) of all samples.

Sample	Gram-negative bacteria					Gram-positive bacteria	
	P. aeruginosa	*Shigella* sp.	*S. enteritidis*	*E. coli*	*K. pneumoniae*	*S. aureus*	*E. faecalis*
Chloramphenicol (positive control)	13.0 ± 0.0	30.0 ± 0.0	29.8 ± 0.0	30.0 ± 0.0	25.9 ± 0.0	25.0 ± 0.0	26.5 ± 0.0
NaCl (negative control)	0	0	0	0	0	0	0
BOMBAX extract (0.25 wt%)	0	0	0	0	0	0	0
$AgNO_3$ (0.025 wt%)	18.0 ± 0.0	11.3 ± 0.0	8.3 ± 0.0	9.9 ± 0.0	9.6 ± 0.0	10.4 ± 0.0	9.8 ± 0.0
AgNP 0.05 wt% BOMBAX extract	18.6 ± 0.8	13.5 ± 0.4	9.3 ± 0.7	12.3 ± 0.6	9.0 ± 0.7	11.7 ± 0.5	10.0 ± 0.3
AgNP 0.10 wt% BOMBAX extract	19.3 ± 0.6	13.6 ± 0.6	10.3 ± 0.4	12.5 ± 0.6	10.0 ± 0.7	11.4 ± 0.4	9.9 ± 1.0
AgNP 0.15 wt% BOMBAX extract	19.4 ± 0.4	14.0 ± 2.6	9.7 ± 0.8	11.8 ± 0.5	10.2 ± 0.1	11.4 ± 0.4	10.6 ± 0.8
AgNP 0.25 wt% BOMBAX extract	19.0 ± 0.0	13.9 ± 1.9	8.9 ± 1.0	11.8 ± 0.2	10.5 ± 0.0	11.3 ± 0.4	10.0 ± 1.4

ogy of the obtained AgNPs. Fig. 5 shows SEM images of the synthesized AgNPs. Structural studies observed by the SEM showed an agglomeration of AgNPs and many lumps or clusters that are characteristic of phytonutrients such as phenolic compounds, flavonoids, waxes, and amino acids. At the lowest BOMBAX concentration of 0.05 wt%, most of the AgNPs were spherical shaped and some flat needles with average sizes of 70 to 80 nm and 300 to 500 nm, respectively, as shown in Fig. 5(AB). Noticeably, SEM images and their magnified images for sizes observed in spherical and quasi-spherical shapes of AgNPs over the whole concentration range of BOMBAX correspond to sizes observed in the size distribution in Table 1. When the concentration of BOMBAX increases to 0.10 wt%, the size and shape of AgNPs are similar to those of the AgNPs synthesized using the previous concentration, except for the additional growth of the needle structured AgNPs, as shown in Fig. 5(CD). The size of the needle structure shown by SEM imaging in Fig. 5(D) was 2 μm. When the concentration of BOMBAX reaches 0.15 wt%, the spherical shape of AgNPs becomes more quasi-spherical with enlarged sizes ranging from 80 to 100 nm (Fig. 5E). Surprisingly, quasi-rectangular and cubic structures of AgNPs on a micrometer scale are observed at this concentration (Fig. 5F). As mentioned earlier, *B. ceiba* L. contains a variety of useful phytochemical compounds that can act as reducing agents

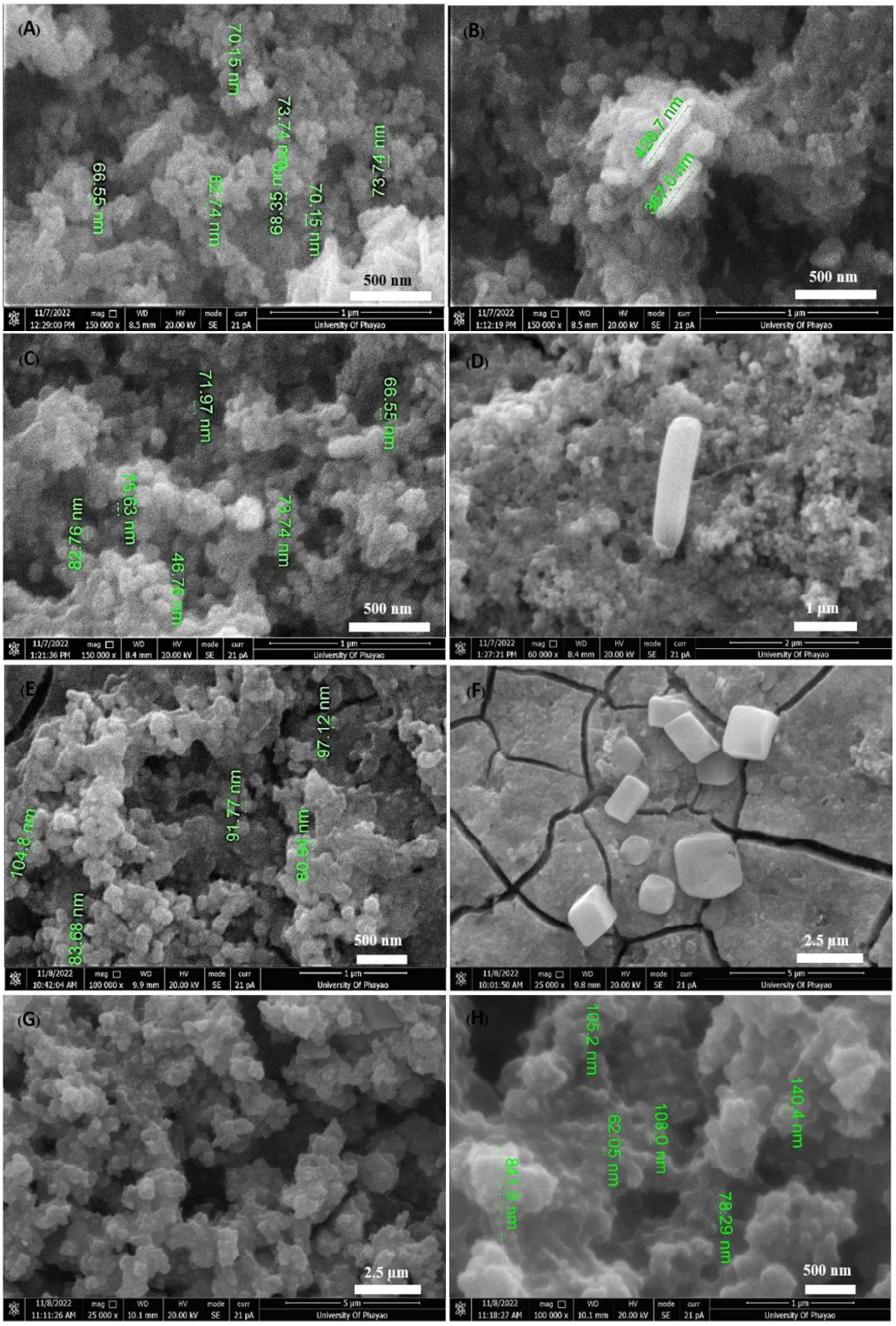

Fig. 5 SEM images of AgNPs (different magnifications of: (A) to (C) 150k X, (D) 60k X, (E) 100k X, (F) and (G) 25k X, and (H) 100k X) prepared using different BOMBAX concentrations of:d (A) and (B) 0.05 wt%, (C) and (D) 0.10 wt%, (E) and (F) 0.15 wt%, and (G) and (H) 0.25 wt%.

and surfactants to control the growth of nanoparticles by behaving as capping agents [36]. The phytochemical compounds of flavonoids and phenolic acids are involved in the reduction process of Ag^+, while xanthones and some carbohydrates can act as capping and stabilizing agents [37, 38]. It has been reported that capping agents act as binding molecules that mainly modulate the surface chemistry, morphology, and size distribution of nanoparticles and maintain the stabilization process [38]. The biogenic capping agents found in various plant extracts used in green synthesis can affect the morphology and size of AgNPs [39, 40]. Therefore, it can be implied that capping agents found in different concentrations of BOMBAX used in this research could have contributed to the different sizes and shapes of the AgNPs. Importantly, there are many research works reporting on the use of surfactants to control the growth of nanoparticles [41, 42]. These findings might explain why the size of AgNPs in this work (approximately 70 to 100 nm observed by SEM for spherical and quasi-spherical shape) does not vary significantly with reference to the concentration range of BOMBAX extract and why some other quasi-rectangular shapes and cubic structures of AgNPs are observed. This is because AgNPs are capped by surfactants found in the phytochemicals in BOMBAX. Finally, when the final concentration of BOMBAX reaches 0.25 wt%, the AgNPs are mostly semi-rectangular and cubic in shape, as shown in Fig. 5(GH). The particle size distribution is in the range of 20 to 260 nm, and their average size is 88 nm, as shown by the mean particle sizes in Table 1.

Antimicrobial activity

The antimicrobial properties of AgNPs have been utilized widely in many industries such as the health, medicinal product, food storage, packaging, wound dressing, textile, and dye reduction industries as well as for environmental applications. In this work, we investigated synthesized AgNPs as antibacterial agents, and antimicrobial activities toward both gram-negative bacteria and gram-positive bacteria were tested compared with chloramphenicol (positive control), NaCl (negative control), and $AgNO_3$ as shown in Table 2. The synthesized AgNPs exhibit good antimicrobial activities toward the tested bacteria. Synthesis of AgNPs using BOMBAX extract at the concentration range between 0.10 wt% and 0.15 wt% is the optimal condition to obtain good antibacterial activity shown as the large inhibition zone observed by the disc diffusion method, which can be explained by the extremely large surface area of AgNPs providing effective binding to the bacterial cell wall or ease of reaching cellular proximity. The decrease in the inhibition zone observed in AgNPs synthesized using 0.25 wt% BOMBAX extract comes from the larger size of AgNPs obtained when using a higher concentration of the extract. Although the BOMBAX extract is assumed to possess antibacterial activities that should be reflected through a greater inhibition zone, it shows no antibacterial activity, which might be due to the medium used in extraction. The inhibition zone diameters (average value ± standard deviation) of the synthesized AgNP samples show superior antibacterial activity (greater inhibition zone) than those of $AgNO_3$ alone, but lower activity (smaller inhibition zone) when compared to chloramphenicol. Surprisingly, the synthesized AgNPs show superior antibacterial activity toward *P. aeruginosa* compared with chloramphenicol and $AgNO_3$. It should be noted that *P. aeruginosa* is a gram-negative bacterium found commonly in the environment causing infections in humans (blood, lungs, and other parts of the body after surgery) and is remarkably capable of resisting antibiotics. [43]. Furthermore, gram-negative bacteria are more resistant than the gram-positive counterparts due to the negatively charged lipopolysaccharide [44]. The superior antimicrobial resistance to *P. aeruginosa* of the synthesized AgNPs will be of advantage for potential use as an antimicrobial agent in health and medicine applications.

CONCLUSION

In this research, AgNPs were successfully synthesized using green synthesis from extract of the flower stamen part of the Cotton Tree (*B. ceiba* L.). Synthesized AgNPs with different BOMBAX concentrations showed various shapes of AgNPs (spherical, quasi-spherical, quasi-rectangular, and cubic structures). The zeta potential values were high, indicating good stability of AgNP colloidal solution after synthesis. The antibacterial effect of synthesized AgNPs predominantly affected the gram-negative bacteria, especially the antibiotic-resistant *P. aeruginosa* which is superior to chloramphenicol. In conclusion, synthesizing AgNPs from the flower stamen part of the Cotton tree is a convenient, cost-effective, and environmentally friendly method to produce a colloidal solution that exhibits good stability with outstanding antibiotic activity toward *P. aeruginosa*.

Acknowledgements: This research project was supported by the Thailand Science Research and Innovation Fund and the University of Phayao (Grant No. FF65-RIM068) and School of Science, University of Phayao (Grant No. PBTSC64012). The authors wish to thank Dr. Chee O. Too for proofreading this manuscript.

REFERENCES

1. Yasien S, Iqbal MM, Javed M, Alnuwaiser MA, Iqbal S, Mahmood Q, Elkaeed EB, Dera AA, et al (2022) Comparative evaluation of various extraction techniques for secondary metabolites from *Bombax ceiba* L. flowering plants along with *in vitro* anti-diabetic performance. *Bioengineering* **9**, 486.

2. Kriintong N, Katisart T (2020) *In vitro* antioxidant and antidiabetic activities of leaf and flower extracts from *Bombax ceiba*. *Pharmacogn Res* **12**, 194–198.
3. Ying S, Guan Z, Ofoegbu PC, Clubb P, Rico C, He F, Hong J (2022) Green synthesis of nanoparticles: current developments and limitations. *Environ Technol Innovation* **26**, 102336.
4. Roy A, Bulut O, Some S, Mandal AK, Yilmaz MD (2019) Green synthesis of silver nanoparticles: biomolecule-nanoparticle organizations targeting antimicrobial activity. *RSC Adv* **9**, 2673–2702.
5. Wypij M, Jędrzejewski T, Trzcińska-Wencel J, Ostrowski M, Rai M, Golińska P (2021) Green synthesized silver nanoparticles: antibacterial and anticancer activities, biocompatibility, and analyses of surface-attached proteins. *Front Microbiol* **12**, 632505.
6. Bharadwaj KK, Rabha B, Pati S, Sarkar T, Choudhury BK, Barman A, Bhattacharjya D, Srivastava A, et al (2021) Green synthesis of gold nanoparticles using plant extracts as beneficial prospect for cancer theranostics. *Molecules* **26**, 6389.
7. Kunoh T, Takeda M, Matsumoto S, Suzuki I, Takano M, Kunoh H, Takada J (2018) Green synthesis of gold nanoparticles coupled with nucleic acid oxidation. *ACS Sustainable Chem Eng* **6**, 364–373.
8. Kausar H, Mehmood A, Khan RT, Ahmad KS, Hussain S, Nawaz F, Iqbal MS, Nasir M, et al (2022) Green synthesis and characterization of copper nanoparticles for investigating their effect on germination and growth of wheat. *PLoS One* **17**, e0269987.
9. Din MI, Arshad F, Hussain Z, Mukhtar M (2017) Green adeptness in the synthesis and stabilization of copper nanoparticles: catalytic, antibacterial, cytotoxicity, and antioxidant activities. *Nanoscale Res Lett* **12**, 638.
10. Sukumar S, Rudrasenan A, Nambiar DP (2020) Green-synthesized rice-shaped copper oxide nanoparticles using *Caesalpinia bonducella* seed extract and their applications. *ACS Omega* **5**, 1040–1051.
11. Akintelu SA, Folorunso AS, Folorunso FA, Oyebamiji AK (2020) Green synthesis of copper oxide nanoparticles for biomedical application and environmental remediation. *Heliyon* **6**, e04508.
12. Saif S, Tahir A, Chen Y (2016) Green synthesis of iron nanoparticles and their environmental applications and implications. *Nanomaterials* **6**, 209.
13. Karunakaran S, Ramanujam S, Gurunathan B (2018) Green synthesised iron and iron-based nanoparticle in environmental and biomedical application: A review. *IET Nanobiotechnol* **12**, 1003–1008.
14. Kiwumulo HF, Muwonge H, Ibingira C, Lubwama M, Kirabira JB, Ssekitoleko RT (2022) Green synthesis and characterization of iron-oxide nanoparticles using *Moringa oleifera*: a potential protocol for use in low and middle income countries. *BMC Res Notes* **15**, 149.
15. Akintelu SA, Oyebamiji AK, Olugbeko SC, Folorunso AS (2021) Green synthesis of iron oxide nanoparticles for biomedical application and environmental remediation: a review. *Ecletica Quim J* **46**, 17–37.
16. Sahin M, Gubbuk IH (2022) Green synthesis of palladium nanoparticles and investigation of their catalytic activity for methylene blue, methyl orange and rhodamine B degradation by sodium borohydride. *React Kinet Mech Catal* **135**, 999–1010.
17. Gulbagca F, Aygün A, Gülcan M, Ozdemir S, Gonca S, Şen F (2021) Green synthesis of palladium nanoparticles: preparation, characterization, and investigation of antioxidant, antimicrobial, anticancer, and DNA cleavage activities. *Appl Organomet Chem* **35**, 6272.
18. Ajitha B, Reddy YA, Reddy PS (2014) Biogenic nanoscale silver particles by *Tephrosia purpurea* leaf extract and their inborn antimicrobial activity. *Spectrochim Acta Part A* **121**, 164–172.
19. Rautela A, Rani J, Debnath (Das) M (2019) Green synthesis of silver nanoparticles from *Tectona grandis* seeds extract: characterization and mechanism of antimicrobial action on different microorganisms. *J Anal Sci Technol* **10**, 5.
20. Melkamu WW, Bitew LT (2021) Green synthesis of silver nanoparticles using *Hagenia abyssinica* (Bruce) J.F. Gmel plant leaf extract and their antibacterial and antioxidant activities. *Heliyon* **7**, e08459.
21. Giri AK, Jena B, Biswal B, Pradhan AK, Arakha M, Acharya S, Acharya L (2022) Green synthesis and characterization of silver nanoparticles using *Eugenia roxburghii* DC. extract and activity against biofilm-producing bacteria. *Sci Rep* **12**, 8383.
22. Taghavizadeh Yazdi ME, Amiri MS, Akbari S, Sharifalhoseini M, Nourbakhsh F, Mashreghi M, Yousefi E, Abbasi MR, et al (2020) Green synthesis of silver nanoparticles using *Helichrysum graveolens* for biomedical applications and wastewater treatment. *BioNanoSci* **10**, 1121–1127.
23. Ranjan P, Das MP, Kumar MS, Anbarasi P, Sindhu S, Sagadevan E, Arumugam P (2013) Green synthesis and characterization of silver nanoparticles from *Nigella sativa* and its application against UTI causing bacteria. *J Acad Ind Res* **2**, 45–49.
24. Alex KV, Pavai PT, Rugmini R, Prasad MS, Kamakshi K, Sekhar KC (2020) Green synthesized Ag nanoparticles for bio-sensing and photocatalytic applications. *ACS omega* **5**, 13123–13129.
25. Chotpatiwetchkul W, Saengsawang M, Sriwong C (2022) Facile and green synthesis of AgNPs by microwave-assisted method using curcumin biomaterial for improving antibacterial activities of NR/Ag composite sheets. *ScienceAsia* **48**, 847–854.
26. Amendola V, Bakr OM, Stellacci F (2010) A study of the surface plasmon resonance of silver nanoparticles by the discrete dipole approximation method: effect of shape, size, structure, and assembly. *Plasmonics* **5**, 85–97.
27. Szerencsés B, Igaz N, Tóbiás Á, Prucsi Z, Rónavári A, Bélteky P, Madarasz D, Papp C, et al (2020) Size-dependent activity of silver nanoparticles on the morphological switch and biofilm formation of opportunistic pathogenic yeasts. *BMC Microbiol* **20**, 176.
28. Zannotti M, Vicomandi V, Rossi A, Minicucci M, Ferraro S, Petetta L, Giovannetti R (2020) Tuning of hydrogen peroxide etching during the synthesis of silver nanoparticles. An application of triangular nanoplates as plasmon sensors for Hg^{2+} in aqueous solution. *J Mol Liq* **309**, 113238.
29. Paramelle D, Sadovoy A, Gorelik S, Free P, Hobley J, Fernig DG (2014) A rapid method to estimate the concentration of citrate capped silver nanoparticles from UV-visible light spectra. *Analyst* **139**, 4855–4861.
30. Alharbi NS, Alsubhi NS, Felimban AI (2022) Green synthesis of silver nanoparticles using medicinal plants:

characterization and application. *J Radiat Res Appl Sci* **15**, 109–124.
31. Bykkam S, Ahmadipour M, Narisngam S, Kalagadda VR, Chidurala SC (2015) Extensive studies on X-Ray diffraction of green synthesized silver nanoparticles. *Adv Nanopart* **4**, 1–10.
32. Ghandehari S, Tabrizi MH, Ardalan P, Neamati A, Shali R (2019) Green synthesis of silver nanoparticles using *Rubia tinctorum* extract and evaluation the anti-cancer properties *in vitro*. *IET Nanobiotechnol* **13**, 269–274.
33. Mehta BK, Chhajlani M, Shrivastava BD (2017) Green synthesis of silver nanoparticles and their characterization by XRD. *J Phys Conf Ser* **836**, 012050.
34. Ofir E, Oren Y, Adin A (2007) Electroflocculation: the effect of zeta-potential on particle size. *Desalination* **204**, 33–38.
35. Ostolska I, Wiśniewska M (2014) Application of the zeta potential measurements to explanation of colloidal $Cr_{(2)}O_{(3)}$stability mechanism in the presence of the ionic polyamino acids. *Colloid Polym Sci* **292**, 2453–2464.
36. Rajput RT (2022) Ethanomedicine and pharmacology of semal (*Bombax ceiba* L.) - a Indian medicinal plant: a review. *Agric Rev* **43**, 145–153.
37. Pradeep M, Kruszka D, Kachlicki P, Mondal D, Franklin G (2022) Uncovering the phytochemical basis and the mechanism of plant extract-mediated eco-friendly synthesis of silver nanoparticles using ultra-performance liquid chromatography coupled with a photodiode array and high-resolution mass spectrometry. *ACS Sustainable Chem Eng* **10**, 562–571.
38. Sidhu AK, Verma N, Kaushal P (2022) Role of biogenic capping agents in the synthesis of metallic nanoparticles and evaluation of their therapeutic potential. *Front Nanotechnol* **3**, 801620.
39. Srikar SK, Giri DD, Pal DB, Mishra PK, Upadhyay SN (2016) Green synthesis of silver nanoparticles: a review. *Green Sustainable Chem* **6**, 34–56.
40. Ahmad S, Munir S, Zeb N, Ullah A, Khan B, Ali J, Bilal M, Omer M, et al (2019) Green nanotechnology: a review on green synthesis of silver nanoparticles – an ecofriendly approach. *Int J Nanomed* **14**, 5087–5107.
41. Chartarrayawadee W, Charoensin P, Saenma J, Rin T, Khamai P, Nasomjai P, Too CO (2020) Green synthesis and stabilization of silver nanoparticles using *Lysimachia foenum-graecum* Hance extract and their antibacterial activity. *Green Process Synth* **9**, 107–118.
42. Heinz H, Pramanik C, Heinz O, Ding Y, Mishra RK, Marchon D, Flatt RJ, Lopis IE, et al (2017) Nanoparticle decoration with surfactants: molecular interactions, assembly, and applications. *Surf Sci Rep* **72**, 1–58.
43. Lister PD, Wolter DJ, Hanson ND (2009) Antibacterial-resistant *Pseudomonas aeruginosa*: clinical impact and complex regulation of chromosomally encoded resistance mechanisms. *Clin Microbiol Rev* **22**, 582–610.
44. Breijyeh Z, Jubeh B, Karaman R (2020) Resistance of gram-negative bacteria to current antibacterial agents and approaches to resolve it. *Molecules* **25**, 1340.